

Supporting Information

Metal-Organic Aerogels Based on Dinuclear Rhodium Paddle-Wheel Units: Design, Synthesis and Catalysis

Baofu Zhu,^a Gang Liu,^a Lianfen Chen,^a Liqin Qiu,^a Liuping Chen,^a Jianyong Zhang,^a Li Zhang,^{*a}
Mihail Barboiu,^{ab} Rui Si,^d and Cheng-Yong Su^{*ac}

^aMOE Laboratory of Bioinorganic and Synthetic Chemistry, Lehn Institute of Functional Materials, School of Chemistry and Chemical Engineering, Sun Yat-Sen University, Guangzhou 510275, China. E-mail: zhli99@mail.sysu.edu.cn; cesscy@mail.sysu.edu.cn

^bInstitut Européen des Membranes—University of Montpellier, ENSCM/UMR CNRS 5635, Place Eugène Bataillon, CC 047, F-34095 Montpellier, France

^cState Key Laboratory of Organometallic Chemistry, Shanghai Institute of Organic Chemistry, Chinese Academy of Sciences, Shanghai 200032, China

^dShanghai Institute of Applied Physics, Chinese Academy Sciences, Shanghai Synchrotron Radiation Facility, Shanghai 201204, China

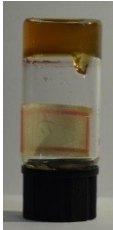

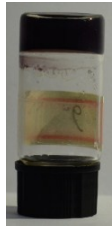
Fax: (+86) 20-8411-5178

E-mail: zhli99@mail.sysu.edu.cn; cesscy@mail.sysu.edu.cn

Contents

Table S1. Gelation tests of H ₃ btctb and Rh ₂ (OAc) ₄ with different reactant concentrations.....	S1
Table S2. Gelation tests of H ₃ btctb and Rh ₂ (OAc) ₄ in different solvents	S2-3
Table S3. Gelation tests of H ₃ btctb and various Rh(II) salt.....	S4
Table S4. Gelation tests of H ₃ btctb and various Rh salts.....	S5
Table S5. Gelation tests of Rh ₂ (OAc) ₄ and various ligands	S6
Figure S1. Wet gel stability tests upon heating.....	S7
Figure S2. Wet gel stability tests in boiled water	S7
Figure S3. Wet gel stability tests in aqueous solutions with different pH	S7
Figure S4. Wet gel stability tests in concentrated HCl	S8
Figure S5. Wet gel stability tests upon shaking	S8
Figure S6. Photographic images of the aerogels.....	S9
Figure S7. EDS spectra of the aerogels.....	S10
Figure S8. TG curves of the aerogels.....	S11
Figure S9. Powder XRD patterns of the aerogels	S12
Figure S10. XPS spectra of the aerogels.....	S13
Figure S11. Solid UV-vis spectra of the aerogels.....	S14
Table S6. EXAFS fitting results of the aerogels.....	S15
Figure S12. EXAFS spectra of the aerogels	S15
Figure S13. The BJH mesopore distribution of the aerogels	S16
Table S7. Recycling Experiments.....	S17
Table S8. C-H Amination of Vinyl Azides Catalyzed by Different Catalysts	S18
ICP Evaluation of the Metal Leaching.....	S19
NMR Data of the Products.....	S20

Table S1. Gelation tests of H₃btctb and Rh₂(OAc)₄ with different reactant concentrations.^a

Entry	H ₃ btctb		C _L ^b	Rh ₂ (OAc) ₄		C _M ^c	Result ^d	MOG Code Photo
	(mmol)	(mg)	(mol/L)	(mmol)	(mg)	(mol/L)		
1	0.015	8.5	0.0075	0.011	4.9	0.0055	G	MOG-Rh-1a 
2	0.030	17.0	0.015	0.0225	10.0	0.011	G	MOG-Rh-1b 
3	0.045	25.5	0.0225	0.034	14.9	0.017	G	MOG-Rh-1c 

^aA 3:4 molar ratio mixture of Rh₂(OAc)₄ and H₃btctb was dissolved in 2 mL of DMF/H₂O (20:1 v/v) with sonication. The resultant homogeneous solution was then left to stand at 85°C for *ca* 50 h. ^bC_L = the concentration of H₃btctb. ^cC_M = the concentration of Rh₂(OAc)₄. ^dG = gel.

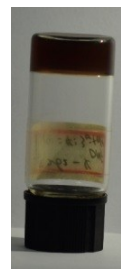
Table S2. Gelation tests of H₃btctb and Rh₂(OAc)₄ in different solvents.^a

Entry	Solvent	Result ^b	Photo
1	DMF (2 mL)	S	
2	DMF (1.975 mL) + H ₂ O (0.025 mL)	S	
3	DMF (1.95 mL) + H ₂ O (0.05 mL)	S	
4	DMF (1.9 mL) + H ₂ O (0.1 mL)	G	
5	DMF (1.95 mL) + CH ₃ OH (0.05 mL)	S	
6	DMF (1.9 mL) + CH ₃ OH (0.1 mL)	G	

7 DMF (1.9 mL) + CH₃CH₂OH (0.1 mL) S

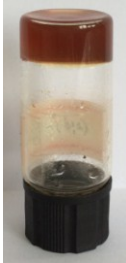



8 DMF (1.5 mL) + CH₃CH₂OH (0.5 mL) G



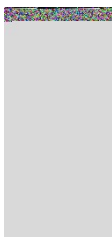
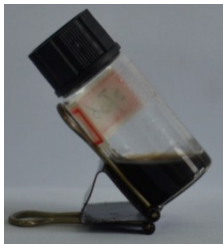

^aA mixture of Rh₂(OAc)₄ (10.0 mg, 0.0225 mmol) and H₃btctb (17.0 mg, 0.030 mmol) was dissolved in 2 mL of DMF/H₂O or DMF/alcohol with sonication. The resultant homogeneous solution was then left to stand at 85°C for *ca* 50 h. ^bG = gel, whereas S = solution.

Table S3. Gelation tests of H₃btctb and various Rh(II) salts.^a

Entry	Molar Ratio (L : M)	H ₃ btctb		Metal salts		Result ^b	MOG Code Photo
		(mmol)	(mmol)	(mg)	(mg)		
1	4:3	0.030	17.0	Rh ₂ (OAc) ₄		G	MOG-Rh-1d
				0.0225	10.0		
2	4:3	0.030	17.0	Rh ₂ (Piv) ₄		G	
				0.0225	14.0		
3	4:3	0.030	17.0	Rh ₂ (TFA) ₄		G	
				0.0225	15.1		

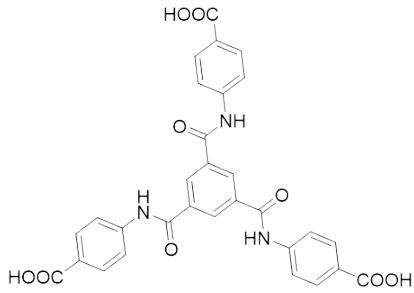
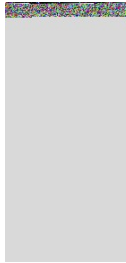
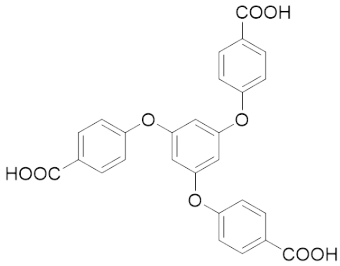

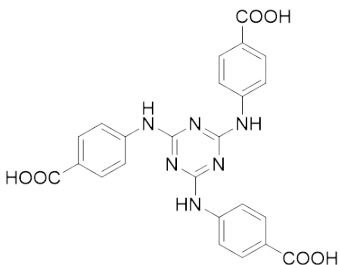

^aA 3:4 molar ratio mixture of an Rh salt and H₃btctb was dissolved in 2 mL of DMF/CH₃OH (1:1 v/v) with sonication. The resultant homogeneous solution was then left to stand at 85°C for *ca* 50 h. ^bG = gel.

Table S4. Gelation tests of H₃btctb and various Rh salts.^a

Entry	Molar Ratio (L : M)	H ₃ btctb		Metal salts		Result ^b	Photo
		(mmol)	(mmol)	(mg)	(mg)		
1	4:3	0.030	17.0	Rh ₂ (OAc) ₄ 0.0225 10.0		G	
2	1:1	0.030	17.0	RhCl ₃ 0.030 6.3		S	
3	2:3	0.030	17.0	[RhCl(COD)] ₂ 0.045 22.2		S	

^aA mixture of an Rh salt and H₃btctb was dissolved in 2 mL of DMF/H₂O (20:1 v/v) with sonication. The resultant homogeneous solution was then left to stand at 85°C for *ca* 50 h. ^bG = gel, whereas S = solution.

Table S5. Gelation tests of Rh₂(OAc)₄ and various ligands.^a

Entry	Ligand Structure	Ligand (mg)	Result ^b	Sample Code Photo
1	<p>H₃btctb</p> 	17.0	G	MOG-Rh-1d 
2	<p>H₃tcpb</p> 	14.0	P	
3	<p>H₃tatab</p> 	14.6	P	

^aA 3:4 molar ratio mixture of Rh₂(OAc)₄ (10.0 mg, 0.0225 mmol) and a tricarboxylic acid (0.030 mmol) was dissolved in 2 mL of DMF/CH₃OH (1:1 v/v) with sonication. The resultant homogeneous solution was then left to stand at 85°C for *ca* 50 h. ^bG = gel, whereas P = precipitate.

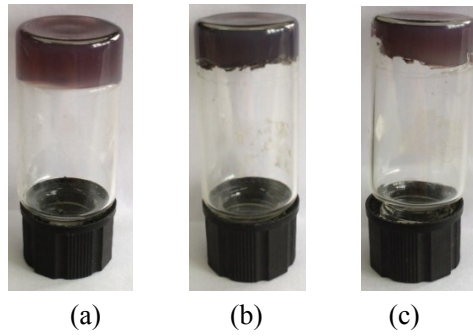


Figure S1. Wet gel stability tests upon heating: (a) before heating, (b) heating at 120°C for 5 min, and (c) heating at 120°C for 10 min.

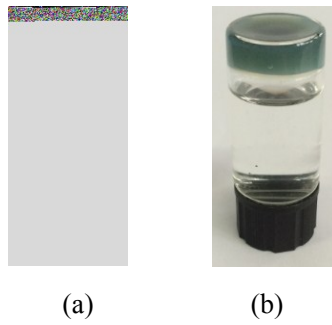


Figure S2. Wet gel stability tests in boiled water: (a) before being immersed in boiled water and (b) after being immersed in boiled water for 3 h.

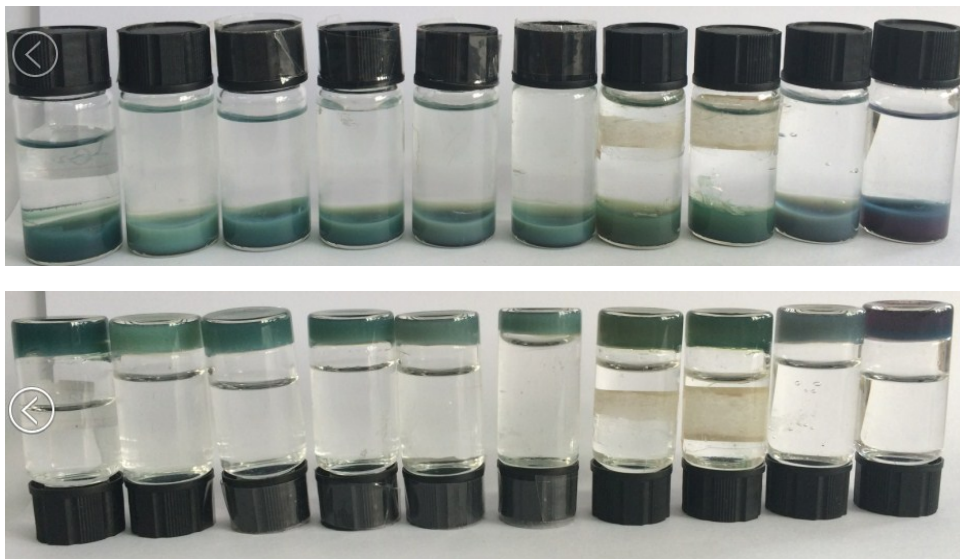


Figure S3. Wet gel stability tests in aqueous solutions with the pH range of 1-10 from left to right).

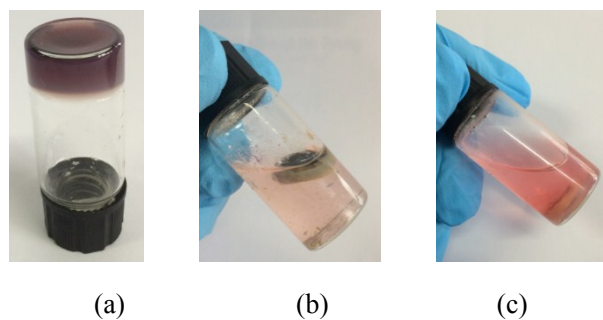


Figure S4. Wet gel stability tests in concentrated HCl (12 M): (a) before being immersed in Conc. HCl, (b) after being immersed in Conc. HCl for 0.5 h, and (b) after being immersed in Conc. HCl for 3 h.

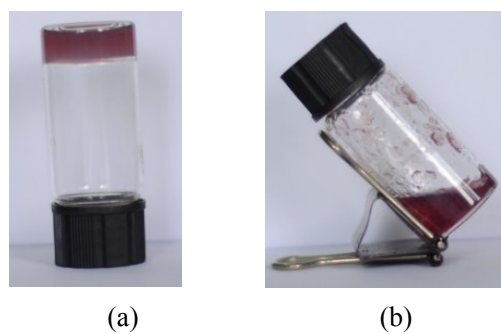


Figure S5. Wet gel stability tests upon shaking: (a) before shaking, and (b) after shaking.

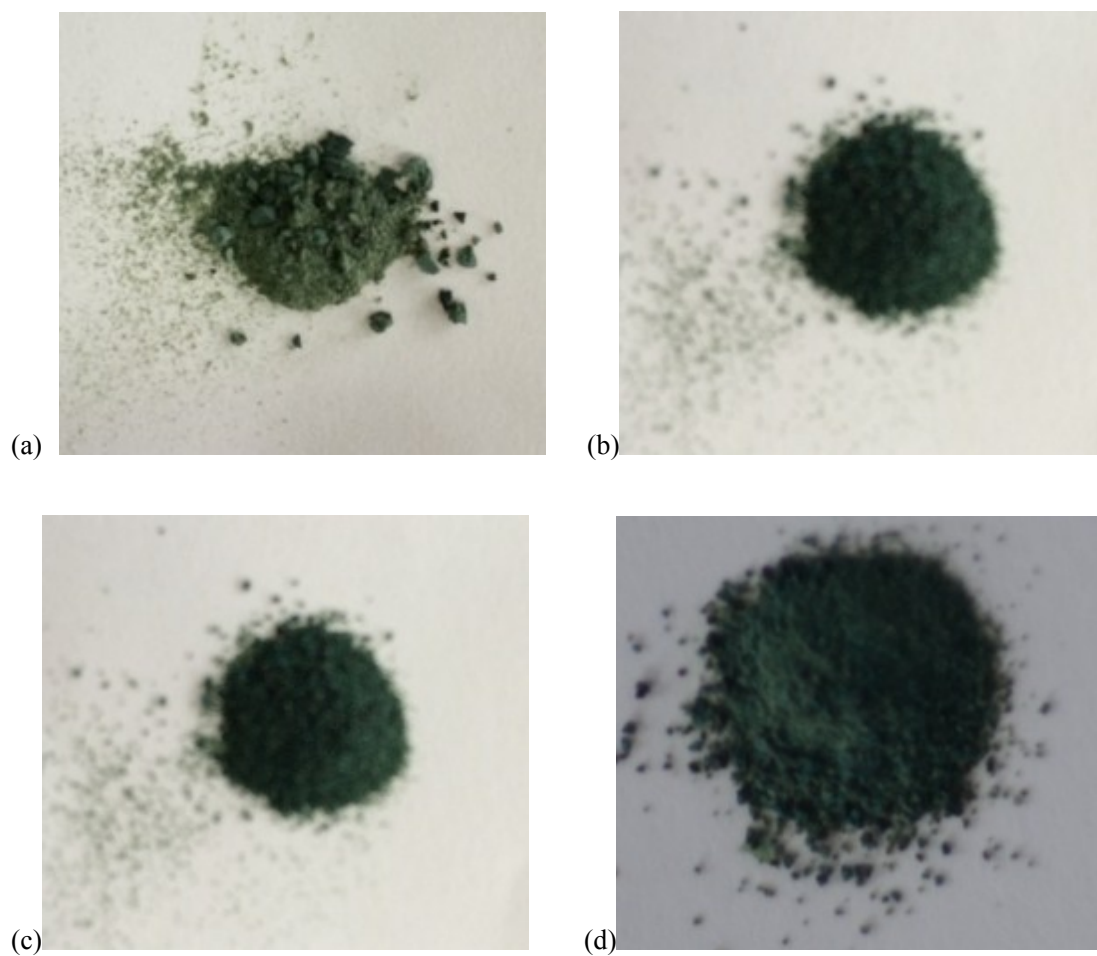


Figure S6. Photographic images of the aerogels: (a) MOA-Rh-1a, (b) MOA-Rh-1b, (c) MOA-Rh-1c, and (d) MOA-Rh-1d.

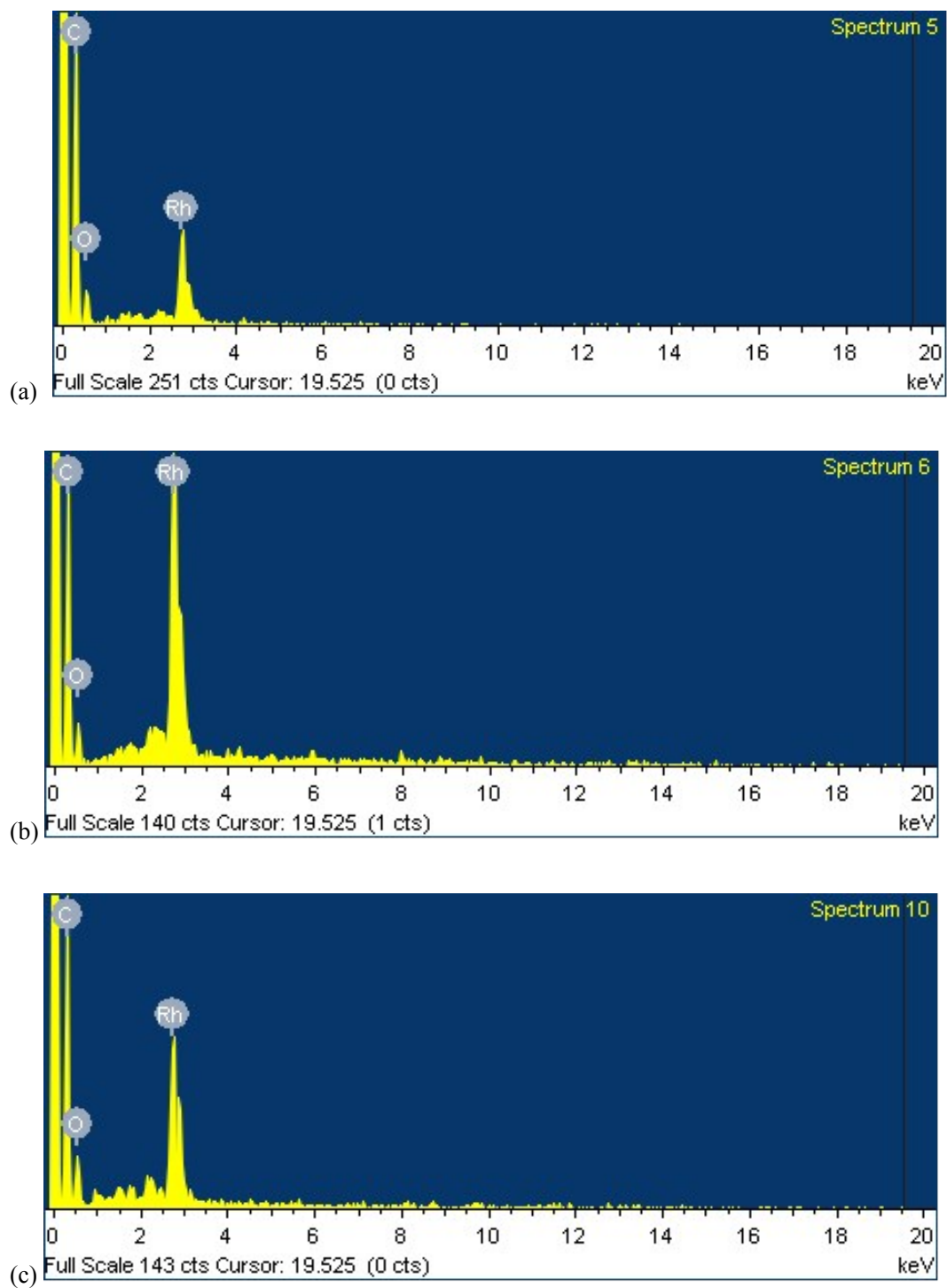
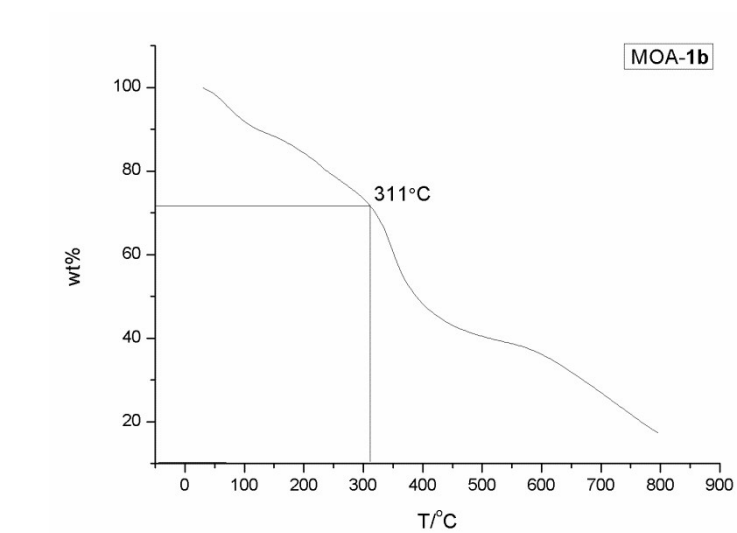
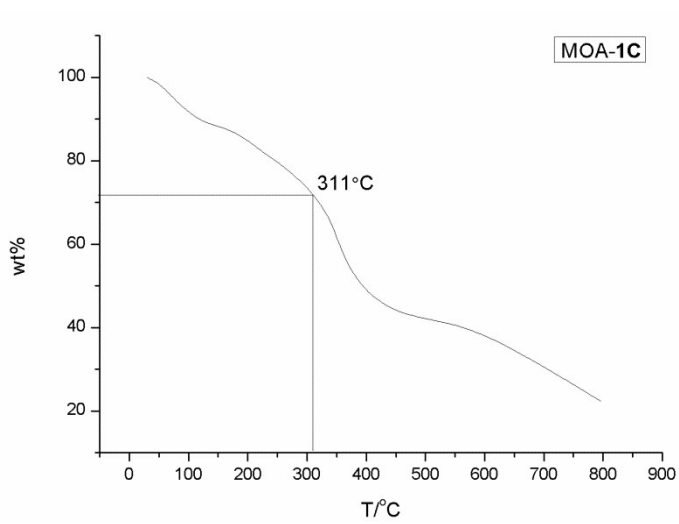


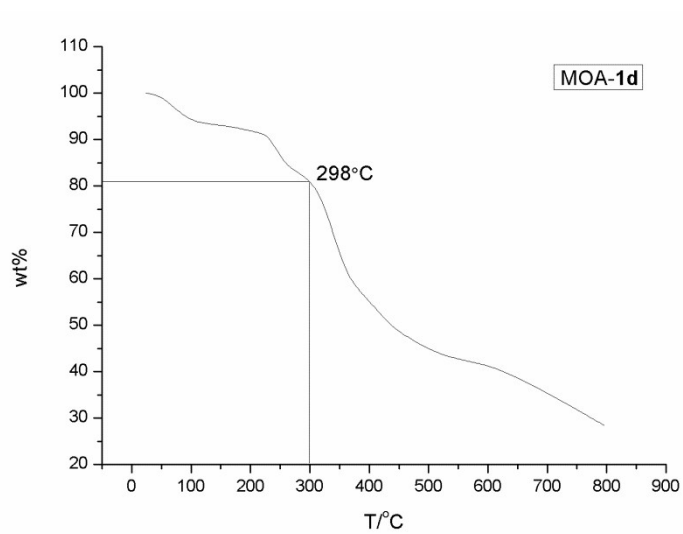
Figure S7. EDS spectra of the aerogels: (a) MOA-Rh-1b, (b) MOA-Rh-1c, and (c) MOA-Rh-1d.



(a)



(b)



(c)

Figure S8. TG curves of the aerogels: (a) MOA-Rh-1b, (b) MOA-Rh-1c, and (c) MOA-Rh-1d.

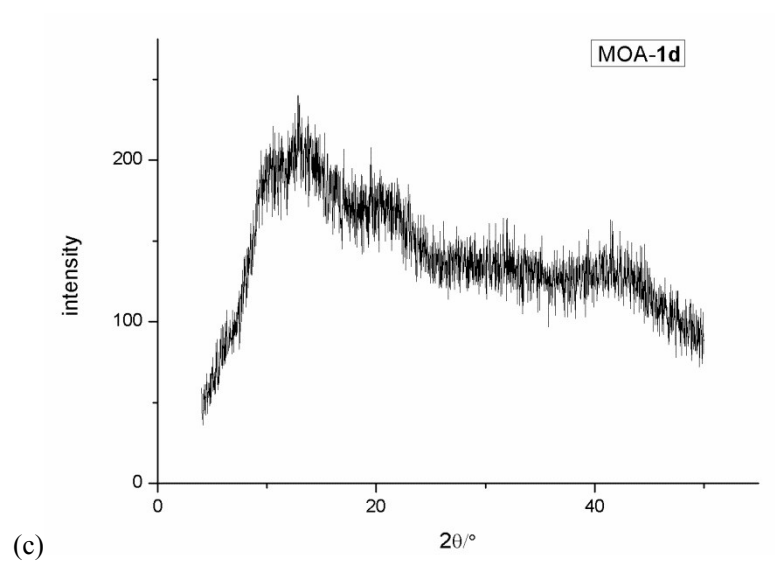
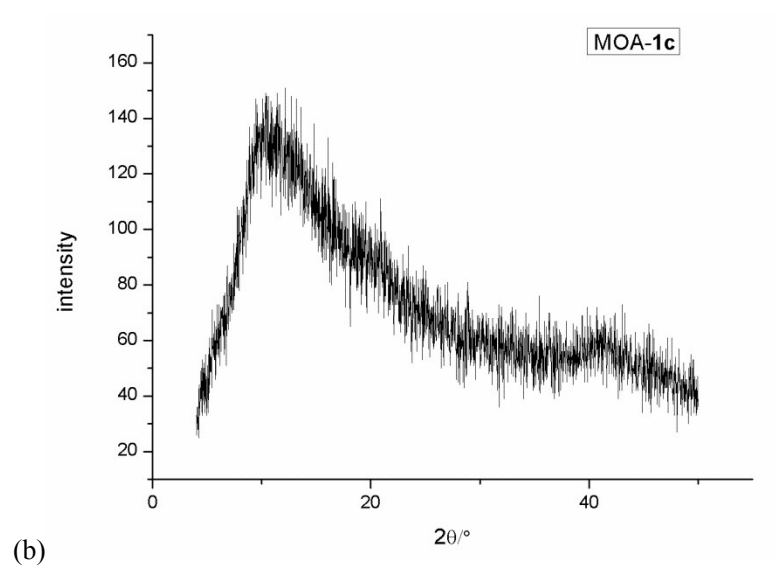
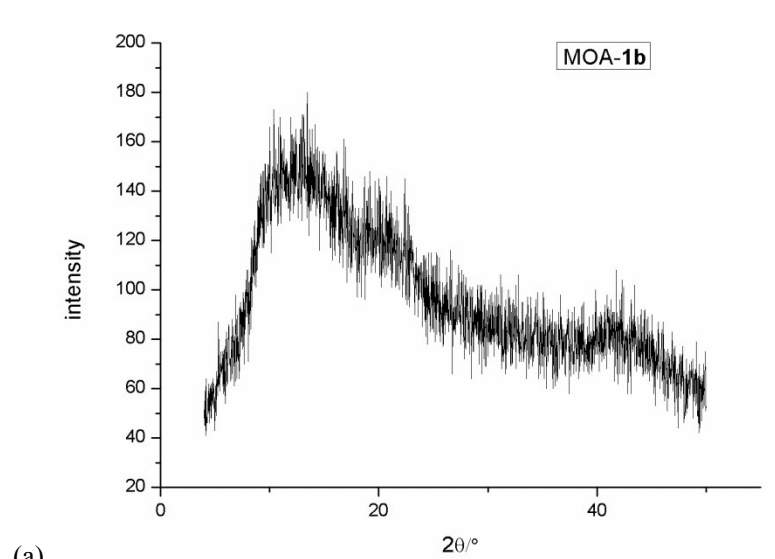


Figure S9. Powder XRD patterns of the aerogels: (a) MOA-Rh-1b, (b) MOA-Rh-1c, and (c) MOA-Rh-1d.

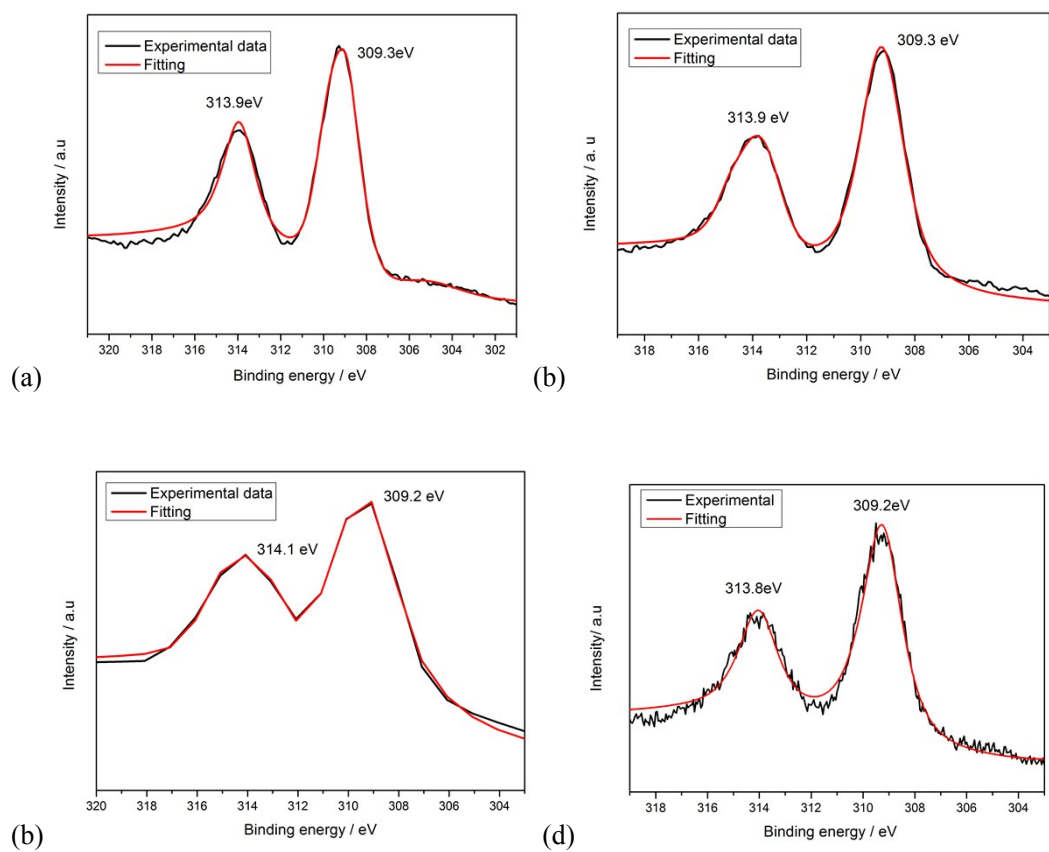


Figure S10. XPS spectra of the aerogels (a) MOA-Rh-1b, (b) MOA-Rh-1c, (c) MOA-Rh-1d before catalysis, and (d) MOA-Rh-1d after catalysis.

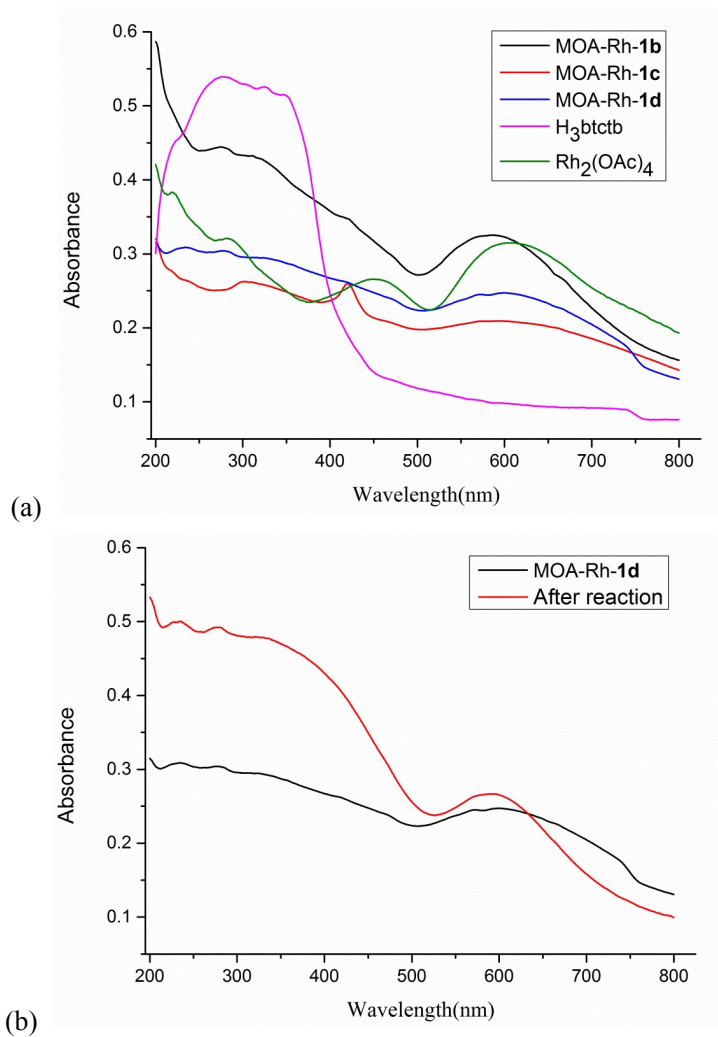


Figure S11. Solid UV-vis spectra of (a) the aerogels MOA-Rh-1b-d, Rh₂(OAc)₄ and H₃btctb, and (b) MOA-Rh-1d before and after catalysis.

The X-ray absorption fine structure (XAFS) spectra at Rh K-edge ($E_0 = 23220$ eV) were performed at BL14W1 beam line of Shanghai Synchrotron Radiation Facility (SSRF) operated at 3.5 GeV under “top-up” mode with a constant current of 240 mA. The XAFS data of MOA-Rh-1d were recorded under transmission mode with high-flux ion chambers. The energy was calibrated accordingly to the absorption edge of pure Rh foil. Athena and Artemis codes were used to extract the data and fit the profiles. For the X-ray absorption near edge structure (XANES) part, the experimental absorption coefficients as function of energies $\mu(E)$ were processed by background subtraction and normalization procedures, and reported as “normalized absorption” to compare with those of standard materials, Rh foil (Rh⁰). For the extended X-ray absorption fine structure (EXAFS) part, the Fourier transformed (FT) data in R space were analyzed by applying the 1st shell approximation model for the Rh-O and Rh-Rh. The passive electron factors, S_0^2 , were determined by fitting the experimental Rh foil data and fixing the Rh-Rh coordination number to be 12, and then fixed for further analysis of the measured samples. The parameters describing the electronic properties (e.g., correction to the photoelectron energy origin, E_0) and local structure environment including coordination number (CN), bond distance (R) and Debye Waller factor around the absorbing atoms were allowed to vary during the fit process. The fitted ranges for k and R spaces were selected to be $k = 3-14 \text{ \AA}^{-1}$ and $R = 1.2-2.5 \text{ \AA}$ (k^3 weighted), respectively.

Table S6. EXAFS fitting results of the dirhodium paddle-wheel units in MOA-Rh-1d.

Sample	Rh-O Bonds		Rh-Rh Bonds		$D. W.$	ΔE_0 (eV)
	R (Å)	CN	R (Å)	CN		
MOA-Rh-1d	2.04±0.01	3.9±0.5	2.40±0.01	0.9±0.2	0.003(O) 0.004(Rh)	3.4±2.6

R , distance between absorber and backscatter atoms; CN , coordination number; $D. W.$, Debye-Waller factor; ΔE_0 , inner potential correction to account for the difference in the inner potential between the sample and the reference compound.

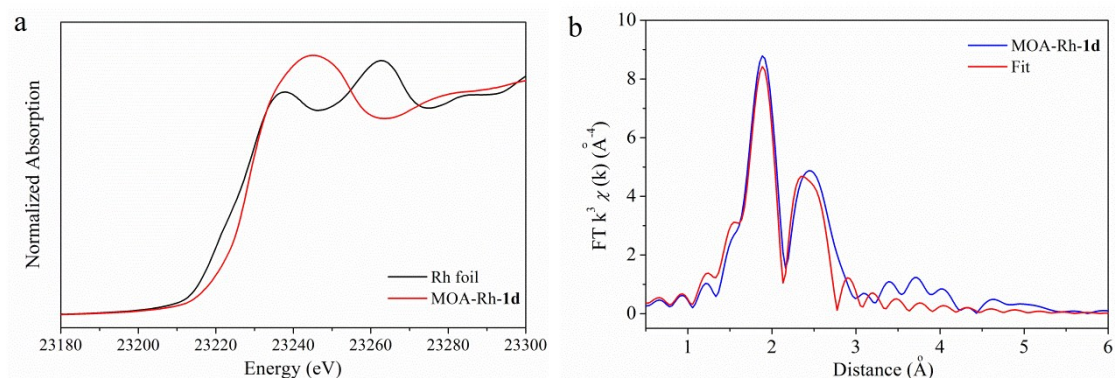
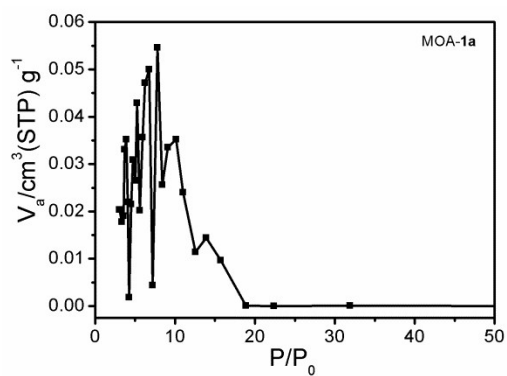
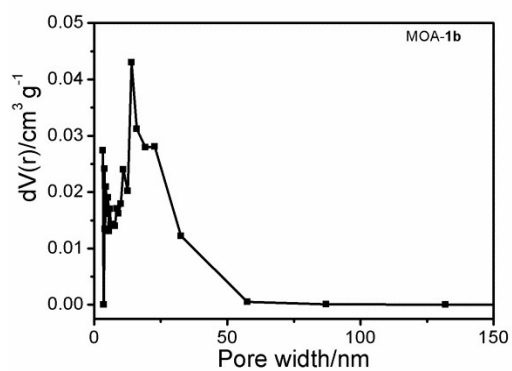


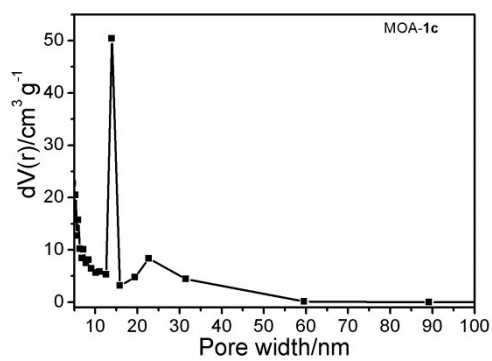
Figure S12. (a) Rh K-edge XANES spectra for Rh-PW and Rh foil. (b) Rh K-edge EXAFS in R space for MOA-Rh-1d with the corresponding fitted curve.



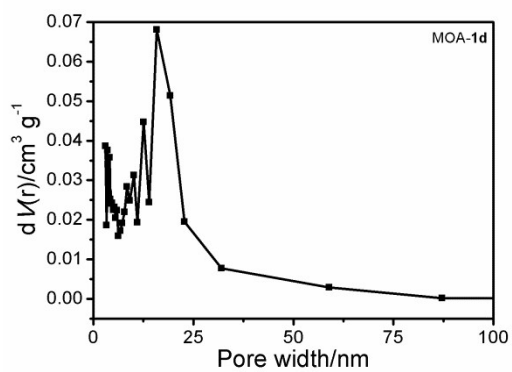
(a)



(b)



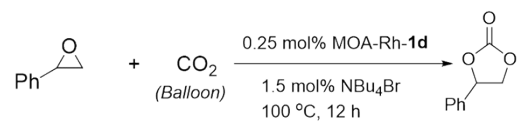
(c)



(d)

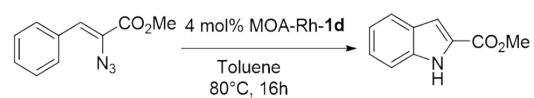
Figure S13. The BJH mesopore distribution of the aerogels: (a) MOA-Rh-1a, (b) MOA-Rh-1b, (c) MOA-Rh-1c, and (d) MOA-Rh-1d.

Table S7a. Recycling experiments of cycloaddition of CO₂ and epoxides



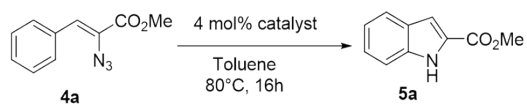
Run	NMR Yield (%)
1	98%
2	91%
3	96%
4	91%
5	95%
6	95%
7	96%
8	94%
9	96%
10	92%

Table S7b. Recycling experiments of C-H amination



Run	Conversion (%)
1	79
2	75
3	81

Table S8. C-H Amination of Vinyl Azides Catalyzed by Different Catalysts.^a



Entry	Catalyst	Yield (%)
1	MOA-Rh- 1d	47%
2 ^b	MOA-Rh- 1d	79%
3	Rh ₂ (OAc) ₄	18%
4	Rh-tcpb	26%
5	Rh-tatab	54%

^aProvided are the conversions of vinyl azides to indoles.

^bThe aerogel MOA-Rh-**1d** was subjected to further solvent exchange with dimethoxyethane (DME) for 3 days and activated by heating at 110 °C under vacuum for 24 h.

ICP Evaluation of the Metal Leaching

To examine the leached Rh content from the aerogel catalyst MOA-Rh-**1d** into the reaction solution, the filtrate was concentrated to dryness. The digestion of the dryness was accomplished with the similar procedure as shown in section 2.3 in the main text. The final clear solution was diluted volumetrically with an aqueous solution of nitric acid (2%) to 10 mL, which was then evaluated by inductively coupled plasma optical emission spectrometer (ICP-OES) for Rh contents.

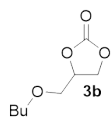
1) As in the catalytic cycloaddition reaction of CO₂ and styrene oxide, the measured Rh content was 0.867 ppm (0.00867 mg), and the leached Rh% should be 0.8%, using the calculation equation “100% × (0.00867 / 1.074 mg)”.

2) As in the catalytic C-H amination of vinyl azide **4a**, the measured Rh content was 0.52 ppm (0.0052 mg), and the leached Rh% should be 0.6%, using the calculation equation “100% × (0.0052 mg / 0.9 mg)”.

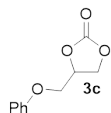
NMR Data of the Products



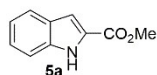
$^1\text{H NMR}$ (400 MHz, CDCl_3) of **3a**: δ 7.40 (m, 3H), 7.36 (m, 2H), 5.68 (t, 1H, $J = 8.0$ Hz), 4.79 (m, 1H), 4.30 (m, 1H).



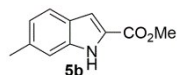
$^1\text{H NMR}$ (400 MHz, CDCl_3) of **3b**: δ 4.75 (br, 1H), 4.41 (m, 1H), 4.28 (m, 1H), 3.54 (dd, 2H, $J = 10.8, 33.6$ Hz), 3.40 (t, 2H, $J = 6.4$ Hz), 1.45 (m, 2H), 1.25 (m, 2H), 0.80 (t, 3H, $J = 7.2$ Hz).



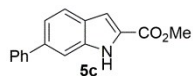
$^1\text{H NMR}$ (400 MHz, CDCl_3) of **3c**: δ 7.32 (t, 2H, $J = 7.2$ Hz), 7.03 (t, 1H, $J = 7.2$ Hz), 6.92 (d, 2H, $J = 7.6$ Hz), 5.04 (br, 1H), 4.61 (m, 1H), 4.53 (m, 1H), 4.19 (dd, 2H, $J = 10.4, 42.8$ Hz).



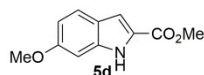
$^1\text{H NMR}$ (400 MHz, CDCl_3) of **5a**: δ 8.98 (br, 1H), 7.68 (d, 1H, $J = 8.0$ Hz), 7.41 (d, 1H, $J = 8.0$ Hz), 7.30 (m, 1H), 7.21 (m, 1H), 7.14 (m, 1H), 3.93 (s, 3H).



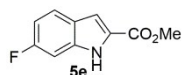
$^1\text{H NMR}$ (400 MHz, CDCl_3) of **5b**: δ 8.92 (br, 1H), 7.33 (d, 1H, $J = 8.4$ Hz), 7.23 (s, 1H), 7.21 (m, 1H), 7.01 (d, 1H, $J = 8.4$ Hz), 3.96 (s, 3H), 2.50 (s, 3H).



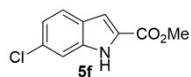
$^1\text{H NMR}$ (400 MHz, CDCl_3) of **5c**: δ 9.11 (br, 1H), 7.74 (d, 1H, $J = 8.0$ Hz), 7.65 (m, 2H), 7.61 (m, 1H), 7.45 (m, 3H), 7.35 (m, 1H), 7.25 (m, 1H), 3.96 (s, 3H).



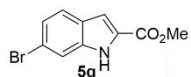
$^1\text{H NMR}$ (400 MHz, CDCl_3) of **5d**: δ 8.99 (br, 1H), 7.57 (m, 1H), 7.28 (s, 1H), 7.19 (m, 1H), 6.86 (m, 1H), 3.95 (s, 3H), 3.88 (s, 3H).



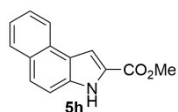
$^1\text{H NMR}$ (400 MHz, CDCl_3) of **5e**: δ 9.14 (br, 1H), 7.64 (m, 1H), 7.22 (m, 1H), 7.11 (m, 1H), 6.95 (m, 1H), 3.97 (s, 3H).



$^1\text{H NMR}$ (400 MHz, CDCl_3) of **5f**: δ 9.17 (br, 1H), 7.62 (d, 1H, $J = 8.4$ Hz), 7.44 (s, 1H), 7.21 (m, 1H), 7.14 (d, 1H, $J = 8.4$ Hz), 3.97 (s, 3H).



$^1\text{H NMR}$ (400 MHz, CDCl_3) of **5g**: δ 9.10 (br, 1H), 7.61 (s, 1H), 7.57 (d, 1H, $J = 8.4$ Hz), 7.28 (d, 1H, $J = 8.4$ Hz), 7.20 (m, 1H), 3.97 (s, 3H).



$^1\text{H NMR}$ (400 MHz, CDCl_3) of **5h**: δ 9.66 (br, 1H), 8.27 (d, 1H, $J = 8.0$ Hz), 7.92 (d, 1H, $J = 8.0$ Hz), 7.78 (m, 1H), 7.73 (d, 1H, $J = 8.8$ Hz), 7.63 (m, 1H), 7.54 (d, 1H, $J = 9.2$ Hz), 7.49 (m, 1H), 4.03 (s, 3H).